

FACILE: Fast, Accurate, and Interpretable Basic-Block Throughput Prediction

Andreas Abel Shrey Sharma Jan Reineke

Saarland University
Saarland Informatics Campus
Saarbrücken, Germany

Abstract

Basic-block throughput models such as uiCA, IACA, GRANITE, Ithemal, llvm-mca, OSACA, or CQA guide optimizing compilers and help performance engineers identify and eliminate bottlenecks. For this purpose, basic-block throughput models should ideally be fast, accurate, and interpretable.

Recent advances have significantly improved accuracy: uiCA, the state-of-the-art model, achieves an error of about 1% relative to measurements across a wide range of microarchitectures. The computational efficiency of throughput models, which is equally important for widespread adoption, especially in compilers, has so far received little attention.

In this paper, we introduce FACILE, an analytical throughput model that is fast, accurate, and interpretable. FACILE analyzes different potential bottlenecks independently and analytically. Due to its compositional nature, FACILE's predictions directly pinpoint the bottlenecks. We evaluate FACILE on a wide range of microarchitectures and show that it is almost two orders of magnitude faster than existing models while achieving state-of-the-art accuracy.

1. Introduction

Basic-block throughput models predict the steady-state throughput of basic blocks on a given microarchitecture. Such models are used by compilers [29, 31, 35, 45–48, 50] to guide optimizations and by performance engineers to pinpoint bottlenecks, which can subsequently be mitigated by code changes or improvements to the microarchitecture.

Ideally, basic-block throughput models should be accurate, efficient, and interpretable:

- The utility of throughput predictions clearly depends on their accuracy. The inaccuracy of models may misguide optimizations and lead to suboptimal performance [32, 36, 37].
- Depending on the use case, the speed of the model is equally important. For example, superoptimizers [29, 35, 45–47] explore a vast space of possible instruction sequences to find the fastest implementation of a given functionality. In such scenarios, the speed of the model is a limiting factor for the overall performance of the superoptimizer.
- Finally, interpretability is important to understand the underlying reasons for the performance of a

basic block, which can help performance engineers or compilers to pick appropriate optimizations.

Recently, several basic-block throughput models have been introduced including uiCA [9], IACA [21], llvm-mca [2, 17], OSACA [27, 28], CQA [13], GRANITE [49], Ithemal [33], and DiffTune [41]. These models offer different trade-offs between accuracy, speed, and interpretability. When it comes to accuracy, the state-of-the-art is defined by uiCA [9], a simulation-based model: On the BHive benchmark suite [15] it achieves an average error of around 1%, while the average error of the other models is about an order of magnitude higher. On the other hand, being simulation-based, uiCA is among the slower models. It is also not straightforward to determine the reasons behind the performance of a basic block from uiCA's cycle-accurate simulation outputs. The fastest available model Ithemal [33], a machine-learned (ML) model, takes about 10 ms on the average to predict the throughput of a basic block, which is an order of magnitude faster than uiCA. However, due to its ML-nature Ithemal is not easily interpretable.

In this paper, we introduce FACILE, a basic-block throughput model that is fast, accurate, and interpretable.

FACILE is based on the following hypothesis: the throughput of a basic block is determined by the maximum of a small set of potential bottlenecks that can be analyzed independently of each other. These potential bottlenecks correspond to pipeline components in the front end and the back end of the microarchitecture, as well as to precedence constraints among instructions in successive loop iterations. We introduce efficient analytical predictors for each of these components, which are combined to predict the throughput of a basic block and to identify the bottlenecks that limit its performance in Section 4.

After briefly discussing FACILE's implementation in Section 5, we extensively evaluate FACILE's accuracy, speed, and interpretability in Section 6. It achieves an average error comparable to uiCA, while being nearly two orders of magnitude faster than Ithemal. It is also more interpretable than both uiCA and Ithemal, as it is based on a simple analytical model. We exploit FACILE's interpretability to gain insights into the evolution of Intel microarchitectures and the impact of individual components on performance.

To summarize, we make the following contributions:

- We introduce FACILE, an analytical basic-block throughput model that is fast, accurate, and interpretable.

- We extensively evaluate FACILE’s accuracy and speed demonstrating that it achieves state-of-the-art accuracy while being almost two orders of magnitude faster than the fastest available models to date.
- As a minor contribution, we exploit FACILE’s interpretability to gain insights into the evolution of Intel microarchitectures.

FACILE is available open source as part of the uiCA repository at <https://github.com/andreas-abel/uiCA>. The Python file `facile.py` acts as the front end to the tool.

2. Related Work

Existing throughput predictors can be broadly classified into three categories: simulation-based, analytical, and learning-based models.

Simulation-based throughput predictors model the complete CPU microarchitecture or parts of it to predict the throughput of a basic block based on cycle-by-cycle simulation. Examples include tools like the uops.info Code Analyzer (uiCA) [9], the LLVM Machine Code Analyzer (llvm-mca) [2, 17], and the Code Quality Analyzer (CQA) [13]. llvm-mca uses the LLVM compiler framework’s [26] scheduling models to predict the performance of machine code. It does not model the front end of a processor pipeline or techniques like macro or micro fusion, which can affect the performance of a basic block. On the other hand, CQA uses a detailed model of the front end of the CPU pipeline, but does not model the back end of the pipeline “because of its complexity and lack of documentation” [13]. Finally, uiCA, the current state-of-the-art in terms of accuracy, models both the front end and the back end of modern Intel CPU pipelines, as well as techniques like macro and micro fusion or move elimination at a high level of detail. FACILE is similar to uiCA in that it models both the front end and the back end of the CPU pipeline, as well as techniques like macro and micro fusion but it does not perform a cycle-by-cycle simulation of the basic block’s execution, rather it considers different pipeline components independently.

To reduce the manual effort that is typically required to set the microarchitecture-specific parameters of simulation-based throughput predictors, DiffTune [41] uses a neural network-based technique to learn the parameters of the llvm-mca simulator automatically. [7] proposes a significantly simpler learning algorithm for the same setting that can serve as a baseline, and showed that DiffTune does not beat this baseline.

Unlike simulation-based basic block throughput predictors, full-system simulators [10–12, 30, 34, 44, 51] model the complete system with all its hardware components and the intricate interactions between them. Such simulators are used to evaluate the performance of entire programs rather than individual basic blocks.

Analytical throughput predictors, such as the Open Source Architecture Code Analyzer (OSACA) [27, 28] and FACILE, in contrast, do not rely on cycle-by-cycle simulation, but use analytical formulas and more coarse-grained models of the microarchitecture for throughput prediction. We note

though that the term “analytical” is broad and analytical models can vary significantly in their level of detail and may even include some form of simulation.

Learning-based throughput predictors use machine learning techniques to predict the throughput of a basic block. They try to alleviate the need for detailed and tedious manual modeling of the microarchitecture and its interactions with the program by learning performance models directly from measured data. Also, learning-based models can in principle be easily adapted to new microarchitectures. Ithemal [33] is one such predictor that uses an LSTM-based neural network to predict the throughput of a basic block. More recently a graph neural network based predictor called GRANITE [49] was proposed. A significant drawback of learning-based predictors is that they are not interpretable. They are often referred to as “black boxes” because it is difficult to understand how they arrive at their predictions. In contrast, FACILE is based on a simple analytical model that is easy to understand and interpret.

To understand the predictions of learning-based predictors, the CoMet [14] framework proposes using post-hoc explanation techniques like the Anchor’s algorithm [42]. The goal being to explain the predictions of a black-box model by identifying instructions in the input basic block that are most relevant to the prediction. Similarly, AnICA [43] uses differential testing and abstract interpretation to generate “abstract basic blocks” that explain inconsistencies between throughput predictors. FACILE primarily provides insights into the impact of individual components of the pipeline on the basic-block performance as opposed to identifying instructions that influence its performance.

3. Background

3.1. Basic-Block Throughput Notions

The reciprocal throughput (also known as the “gap” or the “inverse throughput” in the literature) of a basic block is defined as the number of clock cycles required per iteration of the basic block when it is executed repeatedly in a steady state. As is common in the literature on basic-block throughput prediction, we refer to the reciprocal throughput simply as the “throughput” in the remainder of this paper.

However, this basic definition can be interpreted in different ways depending on the type of basic block that is being considered. Consider a basic block that ends in a branch instruction to the beginning of the block. In this case, “executing the basic block repeatedly” can reasonably be interpreted as executing the basic block repeatedly in an infinite loop. In the following, we will refer to the corresponding notion of throughput as TP_L . On the other hand, consider a basic block that does not end in a branch instruction. In this case, “executing the basic block repeatedly” can reasonably be interpreted as unrolling the basic block for a significant number of iterations. In the following, we will refer to the throughput in this case as TP_U .

It is important to distinguish between TP_L and TP_U , as the pipeline components used by basic blocks are different

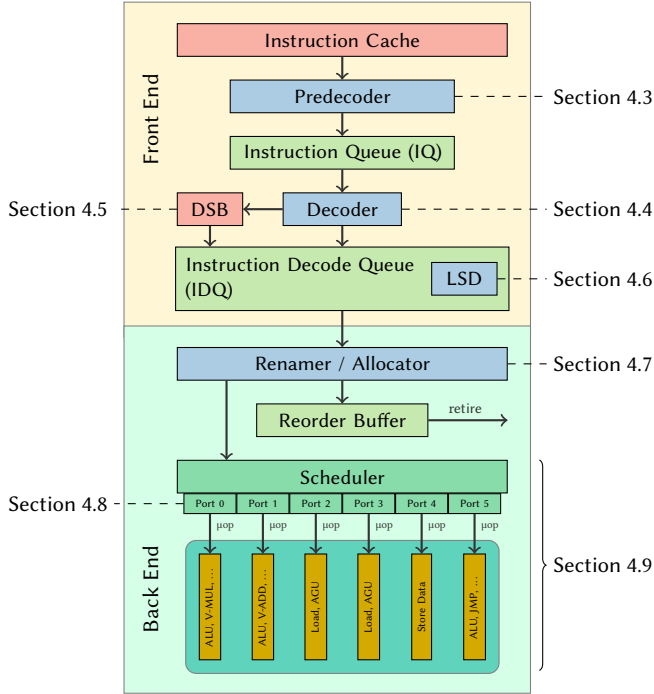


Figure 1: Block diagram of pipeline model.

in these two cases. For a basic block that ends in a branch instruction, in steady state, the decoded μ ops are typically streamed from the μ OP cache (also called Decoded Stream Buffer, short DSB) or the loop stream detector (LSD). Unrolled basic blocks, on the other hand, are typically fetched from the instruction cache (IC) and decoded by the decoders.

Previous work did not always clearly distinguish these two notions of throughput [9]. Intel’s IACA [20] is based on TP_L , and so are OSACA [27, 28] and CQA [13]. On the other hand, Ithemal [33] and DiffTune [41] are based on TP_U . For llvm-mca [2], it is not so clear. As llvm-mca does not model potential bottlenecks in the front end, which is more constrained upon unrolling basic blocks, its predictions can generally be expected to be closer to measurements of TP_L .

In Section 4, we develop two variants of our predictor, one for each notion of throughput.

3.2. High-Level Pipeline Model

Our analytical predictor is based on the pipeline model depicted in Figure 1, which captures the high-level structure of recent Intel Core CPUs.

The pipeline model consists of a front end and a back end. The front end is responsible for fetching and decoding instructions into μ ops, while the back end, also known as the execution engine, is responsible for executing the μ ops, respecting precedence constraints due to read-after-write dependencies, and eventually retiring them.

Both front end and back end can be further divided into multiple components:

- The front end consists of the instruction cache (IC), the predecoder, the decoder, the decode stream buffer (DSB), and the loop stream detector (LSD).
- The back end consists of the renamer, which issues instructions to the scheduler, the scheduler, and the execution units, which are reached via the execution ports.

To enable different components to operate in parallel, buffers are placed between them. For example, the decoder decodes input instructions and stores the resulting μ ops in the instruction decode queue (IDQ). The renamer fetches such μ ops from the IDQ, performs its tasks and stores the μ ops in the reorder buffer while also issuing them to the scheduler. Each pipeline component can process multiple instructions or μ ops in every cycle up to its parallel processing width. As shown in prior work [9], the exact number of μ ops processed by a component in a particular cycle depends on the properties of both the pipeline component and the μ ops processed in that cycle.

Depending on the type of instruction and the state of the pipeline, instructions traverse different pipeline components. In particular, instructions that are part of a loop will usually be processed by the predecoder and decoder only once, and will be served from the LSD or the DSB in subsequent iterations. Instructions that are not part of a loop, in contrast, are usually processed by the predecoder and the decoder. Thus, steady-state throughput predictors for TP_U and TP_L will have to account for different subsets of the pipeline components.

Furthermore, instructions can be merged, split or eliminated at different stages of the pipeline. For example, certain pairs of instructions can be merged in the Instruction Queue (IQ). These instructions are called “macro fused” instructions and they are treated as a single instruction by the rest of the pipeline. Similarly, two μ ops of some instruction types can be fused together in the decoding stage and are treated as a single μ op until they are split either by the renamer or when they enter the scheduler. This is often referred to as “micro fusion”. Before reaching the splitting point, the decoded μ ops are sometimes called *fused-domain* μ ops. Finally, some μ ops can be executed by the renamer itself and are not sent to the scheduler.

3.3. Modeling Assumptions

The actual runtime performance of a basic block depends on a number of factors that are not captured by the pipeline model, some of which are actually impossible to know statically. For example, memory accesses may be served from the L1 cache, the L2 cache, or the main memory, depending on the cache hierarchy and the state of the caches, which may in turn depend on the program’s inputs. Similarly, branches may be predicted correctly or incorrectly. Floating-point operations can take a varying number of cycles depending on the operands, e.g., denormal operands may lead to a greater latency. Loads and stores may or may not alias.

A common assumption in prior work is that basic-block throughput predictors are intended to analyze the performance of *compute-bound* basic blocks. In other words, the

performance of the basic block is limited by the throughput of the front end or back end, and not by the throughput of the memory subsystem or by the branch predictor. As a consequence, a common modeling assumption is that all memory accesses are served from the L1 cache and incur no TLB misses, unaligned loads, or bank conflicts. Similarly, branch mispredictions are assumed to be negligible. We adopt these assumptions in our analytical throughput model. For a more detailed list of commonly unstated assumptions, we refer the reader to [9].

4. FACILE: An Analytical Throughput Model

Our analytical basic-block throughput model FACILE is based on two hypotheses:

- 1) The throughput of a basic block is determined by the slowest pipeline component or by dependency chains between instructions.
- 2) Pipeline components can be analyzed independently from each other, as the pipeline stages are effectively decoupled from each other via buffers.

Under these hypotheses, an accurate throughput predictor can be built from accurate predictors for individual pipeline components and by accounting for dependency chains.

Furthermore, a throughput predictor obtained in this way is naturally interpretable, as it allows to easily identify the bottleneck component(s). It also permits counterfactual reasoning, i.e., it allows to reason about the impact of improving the throughput of a particular pipeline component on the overall throughput.

In the following sections, we will introduce throughput predictors for the following relevant pipeline components:

- Predec: throughput of the predecoder.
- Dec: throughput of the decoder.
- Issue: throughput of the issue stage.
- Ports: maximum throughput due to contention on execution ports.

For benchmarks that are executed as a loop, we also need to bound the throughput of the loop stream detector (LSD) and the decode stream buffer (DSB). In addition, we capture the throughput bound due to precedence constraints among instructions in successive loop iterations (Precedence).

A guiding principle in the design of the component predictors was to make the idealizing (and simplifying) assumption of optimal behavior rather than modeling intricate details of the actual behavior, where this is possible without sacrificing accuracy.

Before introducing all these component predictors, we show how their results can be combined to predict basic-block throughput.

4.1. Throughput Prediction under Unrolling

To predict the throughput of a basic block under unrolling, we determine the maximum throughput among all relevant components:

$$TP_U = \max\{\text{Predec}, \text{Dec}, \text{Issue}, \text{Ports}, \text{Precedence}\} \quad (1)$$

A component is determined to be a *bottleneck* if its throughput matches TP_U . It is common for multiple components to be bottlenecks for a given benchmark.

4.2. Throughput Prediction for Loops

To predict the throughput of a basic block executed as a loop, we determine the maximum of the front-end throughput FE and the throughput of the back-end components:

$$TP_L = \max\{\text{FE}, \text{Issue}, \text{Ports}, \text{Precedence}\} \quad (2)$$

The front-end throughput depends on whether the benchmark is affected by the JCC erratum¹. In that case, neither the LSD nor the DSB are used and the basic block needs to go through the predecoder and the decoder. If the LSD is enabled for the microarchitecture-under-analysis² and the benchmark fits into the instruction decode queue, the throughput is determined by LSD. Otherwise, the benchmark is serviced from the DSB.

$$\text{FE} = \begin{cases} \max\{\text{Predec}, \text{Dec}\} & \text{if benchmark is affected} \\ & \text{by the JCC erratum} \\ \text{LSD} & \text{else if LSD is enabled and} \\ & \#\mu\text{ops} \leq \text{IDQWidth} \\ \text{DSB} & \text{else} \end{cases} \quad (3)$$

4.3. Predecoder

The predecoder fetches instructions from the instruction cache in aligned 16-byte blocks. It detects the beginning of each instruction in these 16-byte blocks and stores the predecoded instructions into the instruction queue (IQ). This is necessary as each instruction can be between 1 to 15 bytes long and finding the beginning of a subsequent instruction may require an inspection of several bytes of the current instruction.

To determine the steady-state behavior of the predecoder, we first determine the number of loop iterations u after which the behavior of the predecoder will start repeating. Let l be the length of the benchmark in bytes. As the predecoder considers blocks of size 16 bytes, the number of iterations u is determined by

$$u = \begin{cases} \frac{lcm(l, 16)}{l} & \text{for unrolling,} \\ 1 & \text{for loops.} \end{cases}$$

Then the throughput of the predecoder can be obtained by computing the number of cycles required to predecode u unrolled copies of the basic block divided by u .

The predecoder can predecode up to five instructions per cycle. If there are more than five instructions in a 16-byte block, the following up to five instructions in the same block are predecoded in the next cycle, and so on. It was shown in

1. As a mitigation to the ‘‘Jump Conditional Code’’ (JCC) erratum, Skylake CPUs do not cache blocks that contain a jump instruction that crosses or ends on a 32-byte boundary [22].

2. On Skylake CPUs it was disabled due to the SKL150 erratum [23].

prior work [9] that when an instruction crosses the 16-byte boundary, depending on whether the nominal opcode of the instruction lies in the first 16-byte block or not, there may be a one cycle penalty in its predecoding. Further, if there are instructions with a length-changing prefix (LCP), the predecoder has to use a special algorithm that results in a penalty of three cycles for every such instruction.

The number of 16-byte blocks in a benchmark of length l that is unrolled u times is $n = \frac{u \cdot l}{16}$. Let $L(b)$ be the number of instruction instances whose last byte is in the b -th 16-byte block. Let $O(b)$ be the number of instruction instances whose first byte of the nominal opcode (i.e., the first byte that does not belong to a prefix) is in the b -th 16-byte block but whose last byte is not in the same block. Then the number of cycles required to predecode all the non-LCP instructions in block b is given by

$$cycle_{NLCP}(b) = \left\lceil \frac{L(b) + O(b)}{5} \right\rceil.$$

Next we add the extra cycles needed due to the penalty for LCP instructions. Let $LCP(b)$ be the number of instruction instances whose first byte of the nominal opcode is in the b -th 16-byte block, and which have a length-changing prefix. Also, let $L(-1) = L(n-1)$, and $O(-1) = O(n-1)$. The number of cycles required to predecode the LCP instructions in block b is given by

$$cycle_{LCP}(b) = \max(0, 3 \cdot LCP(b) - (cycle_{NLCP}(b-1) - 1)).$$

We assume that after the first cycle of predecoding block $b-1$, the predecoder fetches block b and the length-decoding algorithm starts processing the LCP instructions. Hence, we deduct all but one cycle of predecoding block $b-1$ from the penalty of predecoding LCP instructions truncating the difference to zero. Putting everything together, the throughput of the predecoder is predicted as

$$\text{Predec} = \frac{\sum_{b=0}^{n-1} (cycle_{NLCP}(b) + cycle_{LCP}(b))}{u}.$$

For comparison, we also consider a simpler model for the throughput of the predecoder. In this simpler model, we assume that the predecoder predecodes a 16-byte block in each cycle. Hence, for a benchmark of length l bytes, the simple predecoder throughput is given by

$$\text{SimplePredec} = \frac{l}{16}.$$

4.4. Decoder

The decoding unit decodes up to four instructions per cycle and stores the decoded μops into the instruction decode queue (IDQ). The decoding unit consists of three simple decoders and one complex decoder. The complex decoder can decode instructions with up to four μops whereas the simple decoders can only handle instructions with one μop . However, the complex decoder always decodes the first fetched instruction in a cycle. The decoding unit assigns an incoming instruction to a decoder

Algorithm 1: Decoder

```

1  $curDec \leftarrow \#decoders - 1$ 
2  $nAvailableSimpleDecoders \leftarrow 0$ 
3  $nComplexDecInIteration \leftarrow [0, \dots, 0]$ 
4  $firstInstrOnDecInIteration \leftarrow [-1, \dots, -1]$ 
5  $iteration \leftarrow 0$ 
6 while True do
7    $iteration \leftarrow iteration + 1$ 
8    $nComplexDecInIteration[iteration] \leftarrow 0$ 
9   for  $i \in \text{instructions}$  do
10    if  $i$  requires the complex decoder then
11       $curDec \leftarrow 0$ 
12       $nAvailableSimpleDecoders \leftarrow$ 
13         $i.nAvailableSimpleDecoders$  // as
14        provided by uops.info
15    else
16      if  $(nAvailableSimpleDecoders = 0) \vee$ 
17         $((curDec + 1 = \#decoders - 1) \wedge$ 
18         $(i \text{ is macro-fusible}) \wedge$ 
19         $(\text{microarch. cannot decode macro-fusible}$ 
20         $\text{instr. on last decoder}))$  then
21         $curDec \leftarrow 0$ 
22         $nAvailableSimpleDecoders \leftarrow$ 
23         $\#decoders - 1$ 
24      else
25         $curDec \leftarrow curDec + 1$ 
26         $nAvailableSimpleDecoders \leftarrow$ 
27         $nAvailableSimpleDecoders - 1$ 
28      if  $i$  is branch instruction then
29         $nAvailableSimpleDecoders \leftarrow 0$ 
30      if  $curDec = 0$  then
31         $nComplexDecInIteration[iteration] \leftarrow$ 
32         $nComplexDecInIteration[iteration] + 1$ 
33      if  $i$  is the first instruction in the benchmark
34      then
35         $f \leftarrow firstInstrOnDecInIteration[curDec]$ 
36        if  $f \geq 0$  then
37           $u \leftarrow iteration - f$ 
38           $cycles(u) \leftarrow$ 
39           $\sum_{r=f}^{iteration-1} nComplexDecInIteration[r]$ 
40          return  $\frac{cycles(u)}{u}$ 
41        else
42           $firstInstrOnDecInIteration[curDec] \leftarrow$ 
43           $iteration$ 

```

based on the current state of the decoding unit and the properties of the incoming instruction.

Our approach to predict the throughput of the decoding unit is to simulate the allocation of instructions to decoders until the first instruction of the benchmark is allocated to

the same decoder for the second time. At that point, the decoder has reached its steady-state behavior and we can compute the throughput of the decoding unit based on its timing up to that point.

Let u be the number of benchmark iterations between the first and second allocation of the first instruction of the benchmark to the same decoder. Let $cycles(u)$ be the time between these two allocations. Then the throughput of the decoding unit is given by

$$Dec = \frac{cycles(u)}{u}.$$

Algorithm 1 illustrates our approach to computing the throughput of the decoding unit in more detail. The array $nComplexDecInIteration$ stores the number of times the complex decoder is used to decode an iteration of the basic block. This corresponds to the number of cycles needed to decode the basic block in that particular iteration. The array $firstInstrOnDecInIteration$ tracks the decoder that the first instruction in the basic block is allocated to in each iteration. The algorithm iterates over all instructions in the basic block repeatedly and allocates decoders to them (lines 6 to 31) until the first instruction of the benchmark is allocated to the same decoder for the second time (line 26). Then $f = firstInstrOnDecInIteration[curDec]$ is the iteration in which the first instruction of the benchmark was first allocated to the current decoder $curDec$. The number of basic-block iterations between these two allocations is $u = iteration - f$ and the time between these two allocations is $cycles(u) = \sum_{r=f}^{iteration-1} nComplexDecInIteration[r]$.

Similar to the predecoder, we also consider a simpler model for the decoder for comparison. Let n be the number of instructions of the benchmark (ignoring instructions that are macro fused with the preceding instruction). Let c be the number of instructions that require the complex decoder. Let d be the number of decoders in the microarchitecture. Then SimpleDec is given by

$$SimpleDec = \max \left\{ \frac{n}{d}, c \right\}.$$

4.5. Decoded Stream Buffer (DSB)

The decoded stream buffer, also called the μ op cache, stores decoded μ ops. For loops that are bottlenecked by decoding, it can improve the throughput by storing μ ops that are decoded in the first iteration of the loop, forwarding them to the renamer in the subsequent iterations.

We predict the throughput of the DSB simply as the ratio of the number of μ ops in the benchmark to the maximum number of μ ops that can be forwarded from the DSB to the renamer in a single cycle. Let n be the number of (fused-domain) μ ops of the benchmark. Let l be the length (in bytes) of the benchmark. Let w be the width of the DSB. The throughput of the DSB is then given by

$$DSB = \begin{cases} \lceil \frac{n}{w} \rceil & l < 32, \\ \frac{n}{w} & l \geq 32. \end{cases}$$

The first case captures that, after a branch instruction, the CPU cannot load additional μ ops in the same cycle if they are in the same 32-byte block as the branch instruction.

4.6. Loop Stream Detector (LSD)

The loop stream detector detects if a loop's μ ops fit into the IDQ completely. In such situations, it locks the μ ops in the IDQ and continuously streams them to the renamer without waiting for the DSB or the decoders. However, the last μ op of the current loop iteration and the first μ op of the following iteration cannot be streamed in the same cycle. For small loops, this can be a significant bottleneck as the number of μ ops streamed per cycle could be less than the issue width of the microarchitecture. In such cases, the LSD unrolls the loop to increase the number of μ ops streamed per cycle. The number of times the LSD unrolls the loop was reverse engineered in [9].

Let n be the number of (fused-domain) μ ops of the benchmark. Let i be the issue width of the microarchitecture. Let u be the number of times the LSD unrolls the benchmark, as provided at ³. The throughput of the LSD is then given by

$$LSD = \frac{\lceil \frac{n \cdot u}{i} \rceil}{u}.$$

4.7. Issue

As mentioned in Section 3.2, the renamer fetches μ ops from the IDQ and issues them to the scheduler. It is also responsible for allocating resources for loads and stores and assigning execution ports to μ ops. The number of μ ops that can be issued per cycle is bound by the *issue width* of the microarchitecture.

Micro-fused μ ops that are split by the renamer are called *unlaminated* μ ops after being split. They are issued as two μ ops to the scheduler.

We model the throughput of the renamer as the ratio of the number of μ ops issued by the renamer to the issue width of the microarchitecture. Let n be the number of (fused-domain, but after unlamination) μ ops of the benchmark. Let i be the issue width of the corresponding microarchitecture. The throughput is then given by

$$Issue = \frac{n}{i}.$$

Note that LSD dominates Issue in TP_L if the LSD is active, but Issue may be the bottleneck in other cases.

4.8. Execution Ports

Each μ op can be dispatched to a subset of the pipeline's execution ports. Contention on execution ports may slow down the execution of a basic block. Which ports a μ op can be dispatched to has been reverse engineered in [8]. The renamer assigns each μ op to one of the possible execution ports, attempting to evenly distribute μ ops across ports. A precise model of the port-assignment algorithm employed

³ <https://github.com/andreas-abel/uiCA/blob/master/microArchConfigs.py>

by renamers in recent Intel microarchitectures has been described in [9]. In this work, we simply assume that the renamer optimally distributes the load, which is close to reality in most cases. Under this idealizing assumption, [8] previously introduced a linear program to determine the throughput bound due to port contention.

Here, we propose a simpler, more efficient approach that leads to the same bound on all of the BHive benchmarks. Our approach is based on the following observation: If a benchmark contains a subset of μ ops of size u that can collectively be dispatched to port combination pc (i.e., the set of ports that the u μ ops may be dispatched to), then the benchmark’s throughput is limited by $\frac{u}{|pc|}$, as each port accepts at most one μ op per cycle.

Rather than considering every port combination that some subset of a benchmark’s μ ops can be dispatched to, we heuristically consider only port combinations required by pairs of μ ops. Let PC be the set of all port combinations that are used by the μ ops of a benchmark, and let $PC' = \{pc \cup pc' \mid pc, pc' \in PC\}$ be the set of port combinations of pairs of μ ops in the benchmark. Then we predict the throughput bound Ports due to port contention as follows:

$$\text{Ports} = \max_{pc \in PC'} \left\{ \frac{u}{|pc|} \mid \begin{array}{l} u = \text{number of } \mu\text{ops in benchmark} \\ \text{whose port combination is a subset of } pc \end{array} \right\}$$

We exclude μ ops from instructions that may be eliminated or that are macro-fused with preceding instructions. To provide interpretable feedback in case Ports is a bottleneck component, we can extract the instructions whose μ ops experience the maximal port contention.

4.9. Precedence Constraints

In the steady state, the throughput of a basic block may be limited by precedence constraints of instructions across basic-block iterations due to read-after-write dependencies.

To determine the bound on the throughput due to such constraints, we construct a weighted directed dependence graph. The nodes of this graph correspond to the values consumed and produced by the instructions of the benchmark. For each instruction, we create a node for each value it consumes and each value it produces. These nodes are then connected by edges that capture the latency between the consumption of the source value and the production of the target value. We obtain the necessary data for this construction from uops.info [8].

We add 0-latency edges between produced and consumed values to capture the dependencies between instructions of the benchmark. This includes dependencies within a single iteration of the basic block as well as between consecutive iterations of the basic block. Such dependency edges are associated with an iteration count. This iteration count is 0 for intra-iteration dependencies and 1 for inter-iteration dependencies. The iteration count of all edges capturing instruction latencies is 0.

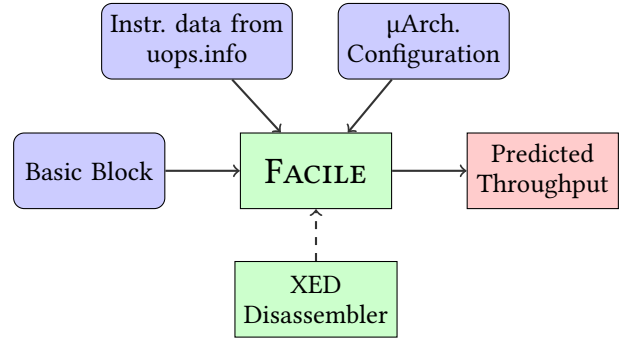


Figure 2: Flow diagram of FACILE.

Now consider a cycle through such a dependence graph. The sum of the latency weights of the edges on this cycle is the latency of the cycle. The sum of the iteration counts of the edges on this cycle is the number of iterations the cycle spans. The throughput bound due this particular cycle is the ratio of the latency to the number of iterations. The throughput bound of the benchmark as a whole is the maximum such ratio across all cycles through the graph. Note that by construction any cycle must include at least one inter-iteration edge and so the iteration count is at least one. This ratio can be obtained using optimum cycle ratio algorithms [16]. Our implementation employs Howard’s value iteration algorithm [16, 18] to compute it.

To provide interpretable feedback in case Precedence is a bottleneck component, we can extract the dependency chain that exhibits the maximal latency.

Our approach is reminiscent of similar analyses in the context of *modulo scheduling* [19, 25, 38], where precedence constraints induce a *recurrence-constrained minimum initiation interval* between successive loop iterations, which corresponds to the throughput bound we compute here. Modulo scheduling also accounts for resource constraints, which correspond to the throughput bounds induced by the various pipeline components in our approach and discussed in previous sections.

5. Implementation

FACILE is implemented in Python 3. It takes a basic block binary as input and returns its predicted throughput. To this end, the binary is first disassembled using a modified version of the Intel X86 Encoder Decoder (XED) library, which provides a Python interface and is provided at ⁴. Then, the throughput of the basic block is predicted using the model described in Section 4. The throughput depends both on high-level parameters of the microarchitecture, such as the issue width, the DSB width, or the number of decoders, as well as on properties of individual instructions, such as their port mapping and latency. For this information, FACILE relies on two sources:

4. <https://github.com/andreas-abel/XED-to-XML>

- 1) Microarchitecture-specific parameters are obtained from the microarchitecture configuration files from uiCA [4].
- 2) Instruction-specific parameters are obtained from the uops.info database [6, 8].

The basic flow of FACILE is depicted in Figure 2. FACILE can be invoked from the command line or by calling the predictor function from other Python scripts, which is how we use it in our experiments.

6. Experimental Evaluation

In this section, we experimentally evaluate three different aspects of FACILE:

- **Accuracy:** We compare the accuracy of FACILE to that of other throughput predictors and analyze the impact of the various components on its accuracy.
- **Computational efficiency:** We analyze the efficiency of FACILE by comparing it to that of other throughput predictors as well as measuring the contribution of individual components to the execution time of FACILE.
- **Interpretability:** We exploit its interpretability to gain insights into the evolution of Intel microarchitectures.

6.1. Benchmarks

The BHive [15] benchmark suite is often used for evaluating throughput predictors for basic blocks. It is an open-source benchmark suite with more than 300,000 basic blocks that have been extracted from applications from different domains such as numerical computing, databases, compilers, machine learning and cryptography. However, as pointed out by prior work [9], there are two important issues with the BHive benchmark suite. First, there are basic blocks in the BHive suite that do not adhere to the modeling assumptions discussed in Section 3.3. Second, the benchmarks in the BHive suite do not end in branch instructions. Hence, the measurements made by the BHive profiler are based on the TP_U notion of throughput while most previous predictors use the TP_L notion of throughput.

To address these issues, we use a modified version of the BHive benchmarks as obtained from [5]. It contains a subset of the BHive benchmarks that conforms to the modeling assumptions from Section 3.3. Furthermore, it also contains variants of the benchmarks from the BHive suite that end in a branch instruction. This allows for a more meaningful comparison with predictors that are based on the TP_L notion of throughput.

We refer to the benchmarks based on the TP_U notion of throughput as $BHive_U$ and those based on the TP_L notion as $BHive_L$ in the remainder of this work.

6.2. Accuracy

In this section, we study the accuracy of FACILE. We compare its accuracy to that of other throughput predictors on all modern Intel Core microarchitectures listed in Table 1.

As prior work [9, 15, 41], we use the following metrics to compare the accuracy of the throughput predictors:

TABLE 1: Microarchitectures used for the evaluation.

μ Arch	Abbr.	Released	CPU
Rocket Lake	RKL	2021	Intel Core i9-11900
Tiger Lake	TGL	2020	Intel Core i7-1165G7
Ice Lake	ICL	2019	Intel Core i5-1035G1
Cascade Lake	CLX	2019	Intel Core i9-10980XE
Skylake	SKL	2015	Intel Core i7-6500U
Broadwell	BDW	2015	Intel Core i5-5200U
Haswell	HSW	2013	Intel Xeon E3-1225 v3
Ivy Bridge	IVB	2012	Intel Core i5-3470
Sandy Bridge	SNB	2011	Intel Core i7-2600

- **Mean Absolute Percentage Error (MAPE):** The mean absolute percentage error of the predictions made by the throughput predictor, relative to the measured throughputs. For a set of pairs of measured and predicted throughput values, $S = \{(m_i, p_i)\}_{i=1}^n$, the MAPE is defined as:

$$MAPE(S) = \frac{1}{n} \sum_{i=1}^n \left| \frac{m_i - p_i}{m_i} \right|$$

- **Kendall’s tau coefficient [24]:** Kendall’s tau is a measure of the correlation between two rankings. We use Kendall’s tau to compare pairs of benchmarks based on their throughput. As mentioned by prior works [9, 15], for certain applications, the relative ordering of different basic blocks based on their throughput is more important than the absolute throughput values.

For our comparison, we use the most recent version of the throughput predictors wherever possible. We use OSACA [28] at version 0.5.0, llvm-mca [2] at version 15.0.7 and CQA [1] at version 2.17.0. Additionally, since DiffTune is based on llvm-mca 8.0.1, we also include a comparison with this version of llvm-mca. For DiffTune [41], we use the version at [39] with the models from the paper that are available at ⁵. “learning-bl” corresponds to the baseline for evaluating llvm-mca parameter learning approaches proposed in [7]; we use the code and models that are available at [3]. We use IACA [21] at versions 3.0 and 2.3 as version 3.0 does not support the older microarchitectures. We use Ithemal [33] at [40] and uiCA [9] at [4]. We could not experimentally evaluate GRANITE [49] as the trained model is not publicly available. We execute all the throughput predictors with a timeout of one hour. If a throughput predictor crashes or does not terminate within the timeout, we report a throughput of zero for that benchmark. We round the predictions to two decimal digits as the measurements were rounded in the same way.

FACILE versus other predictors. Table 2 shows the MAPE and Kendall’s tau for our experiments on the $BHive_U$ and $BHive_L$ benchmarks. For completeness, we evaluate all throughput predictors on both $BHive_U$ and $BHive_L$ benchmarks. For predictors based on the TP_L notion of

5. <https://github.com/ithemal/DiffTune/issues/1>

TABLE 2: Comparison of predictors on $BHive_U$ and $BHive_L$.

μ Arch	Predictor	$BHive_U$		$BHive_L$	
		MAPE	Kendall	MAPE	Kendall
RKL	FACILE	0.42%	0.9860	1.04%	0.9731
	uiCA	0.49%	0.9835	0.92%	0.9755
	llvm-mca-15	25.84%	0.6553	15.20%	0.8380
	CQA 2.17.0	19.18%	0.7085	5.69%	0.9123
TGL	FACILE	1.15%	0.9717	1.62%	0.9617
	uiCA	0.97%	0.9769	0.98%	0.9731
	llvm-mca-15	25.92%	0.6989	13.98%	0.8389
	CQA 2.17.0	21.76%	0.6996	5.44%	0.9139
ICL	FACILE	1.17%	0.9713	1.36%	0.9681
	uiCA	1.00%	0.9771	0.77%	0.9759
	OSACA	20.11%	0.7032	10.07%	0.7865
	llvm-mca-15	25.55%	0.6970	13.64%	0.8512
	CQA 2.17.0	21.82%	0.6982	5.03%	0.9256
CLX	FACILE	0.62%	0.9692	1.24%	0.9720
	uiCA	0.45%	0.9713	0.65%	0.9825
	llvm-mca-15	23.17%	0.7211	13.21%	0.8060
	OSACA	19.02%	0.7910	10.61%	0.8350
SKL	FACILE	0.69%	0.9753	1.08%	0.9752
	uiCA	0.45%	0.9798	0.38%	0.9895
	Ithema1	8.28%	0.8172	13.66%	0.7582
	IACA 3.0	13.49%	0.7802	14.26%	0.8290
	IACA 2.3	11.85%	0.8071	8.42%	0.8477
	OSACA	14.04%	0.7810	10.04%	0.8223
	llvm-mca-15	15.61%	0.7258	12.01%	0.8015
	llvm-mca-8	15.39%	0.7434	11.98%	0.8021
	DiffTune	24.48%	0.6626	104.88%	0.6426
	learning-bl	12.02%	0.7933	15.63%	0.8020
	CQA 2.17.0	16.07%	0.7375	6.58%	0.8972
BDW	FACILE	0.73%	0.9852	1.44%	0.9704
	uiCA	1.08%	0.9805	0.60%	0.9841
	IACA 3.0	14.69%	0.8012	11.47%	0.8725
	IACA 2.3	13.22%	0.8206	5.84%	0.8928
	OSACA	17.00%	0.7621	8.95%	0.8528
	llvm-mca-15	14.23%	0.7793	16.71%	0.8286
	CQA 2.17.0	16.11%	0.7593	5.00%	0.9222
HSW	FACILE	1.26%	0.9791	1.50%	0.9690
	uiCA	0.76%	0.9850	0.59%	0.9842
	Ithema1	7.38%	0.8400	16.19%	0.7700
	IACA 3.0	15.04%	0.8080	12.00%	0.8733
	IACA 2.3	13.13%	0.8291	5.79%	0.8925
	OSACA	17.49%	0.7644	9.06%	0.8517
	llvm-mca-15	20.29%	0.7835	18.97%	0.8259
	llvm-mca-8	21.08%	0.7784	19.46%	0.8171
	DiffTune	24.80%	0.6997	138.47%	0.6925
	learning-bl	11.82%	0.8302	19.26%	0.8052
	CQA 2.17.0	16.23%	0.7668	5.05%	0.9229
IVB	FACILE	1.80%	0.9568	1.52%	0.9624
	uiCA	1.50%	0.9609	1.11%	0.9495
	Ithema1	7.08%	0.8212	12.43%	0.7785
	IACA 2.3	13.94%	0.7739	11.54%	0.8271
	OSACA	23.87%	0.6388	15.80%	0.7467
	llvm-mca-15	22.79%	0.7656	20.76%	0.8154
	llvm-mca-8	22.93%	0.7622	20.76%	0.8138
	DiffTune	26.21%	0.6470	82.94%	0.7516
	learning-bl	13.20%	0.7654	16.89%	0.7937
	CQA 2.17.0	40.60%	0.5167	4.05%	0.9174
SNB	FACILE	1.95%	0.9586	1.33%	0.9742
	uiCA	1.91%	0.9613	0.98%	0.9650
	IACA 2.3	11.91%	0.8194	9.95%	0.8482
	OSACA	12.63%	0.7939	13.08%	0.8137
	llvm-mca-15	22.67%	0.8069	18.34%	0.8455
	CQA 2.17.0	32.94%	0.6274	4.07%	0.9238

TABLE 3: Influence of components on the prediction accuracy for Rocket Lake, Skylake, and Sandy Bridge.

	Predictor	$BHive_U$		$BHive_L$	
		MAPE	Kendall	MAPE	Kendall
RKL	FACILE	0.42%	0.9860	1.04%	0.9731
	FACILE w/ SimplePredec	4.38%	0.9024		
	FACILE w/ SimpleDec	0.69%	0.9836		
	only Predec	14.84%	0.7291		
	only Dec	26.37%	0.6840		
	only DSB			100.00%	0.0078
	only LSD			24.26%	0.6505
	only Issue	41.45%	0.6774	29.85%	0.6520
	only Ports	29.18%	0.5122	26.40%	0.7132
	only Precedence	88.56%	0.3589	22.55%	0.4428
	only Predec+Ports	9.36%	0.8399		
	only Precedence+Ports	22.40%	0.6149	6.59%	0.8467
	FACILE w/o Predec	9.02%	0.8512		
	FACILE w/o Dec	1.19%	0.9734		
	FACILE w/o DSB			1.04%	0.9731
	FACILE w/o LSD			2.52%	0.9556
FACILE w/o Issue	0.43%	0.9857	1.06%	0.9724	
FACILE w/o Ports	7.88%	0.8570	7.90%	0.8002	
FACILE w/o Precedence	5.36%	0.8853	14.88%	0.7967	
SKL	FACILE	0.69%	0.9753	1.08%	0.9752
	FACILE w/o DSB			2.70%	0.9629
	FACILE w/o Issue	0.76%	0.9736	4.34%	0.9107
SNB	FACILE	1.95%	0.9586	1.33%	0.9742
	FACILE w/ SimpleDec	3.76%	0.9378		

throughput, we present the $BHive_U$ results in gray and vice versa for the predictors based on TP_U .

The main finding is that FACILE performs similarly to or slightly worse than the state-of-the-art uiCA on all microarchitectures, but significantly better than all other throughput predictors. We also note that the gap between FACILE and uiCA is generally smaller on $BHive_U$ than on $BHive_L$.

Although we were unable to run GRANITE ourselves, based on the results reported in the paper [49] for the BHive benchmark suite, we note that FACILE significantly outperforms GRANITE on all microarchitectures.

Figure 3 shows heatmaps relating the measured and predicted throughputs for $BHive_L$ benchmarks with a measured throughput of less than 10 cycles on Rocket Lake.

The key takeaway from Figure 3 is that both FACILE and uiCA are able to predict the throughput of most benchmarks with a high accuracy. We also note that FACILE is always optimistic in its predictions, i.e., it always predicts a higher throughput than the measured throughput.

Influence of FACILE’s components on accuracy.

Next, we study the importance of each component of FACILE for the purpose of accurate throughput prediction. Table 3 shows the MAPE and Kendall’s tau for the different variants of FACILE on both $BHive_U$ and $BHive_L$ benchmarks for Rocket Lake, Skylake, and Sandy Bridge. Note that for components that are not used by TP_U or TP_L , the corresponding cells in the table are empty.

First, consider the experiments where we replace individual components of FACILE with simpler versions. Under Rocket Lake, replacing Predec with SimplePredec leads

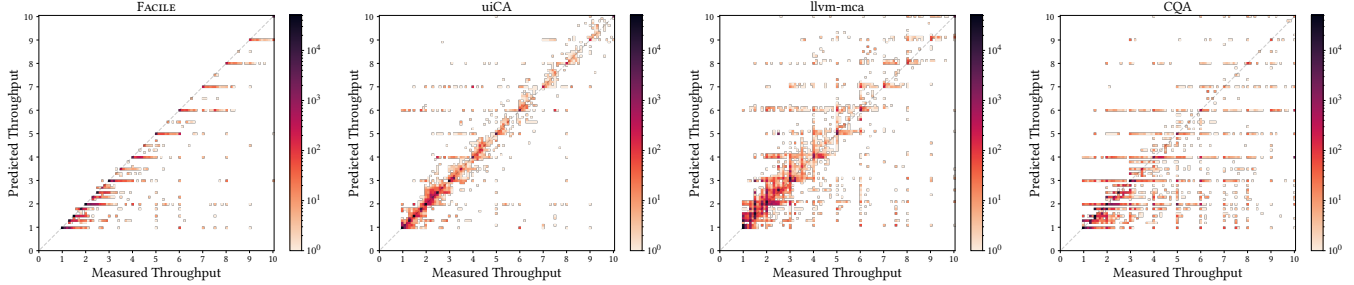


Figure 3: Heatmaps for $BHive_L$ for basic blocks with a measured throughput of less than 10 cycles/iteration on Rocket Lake

to a significant drop in accuracy, which shows that the more complex Predec is required for accurate throughput prediction. Replacing Dec by SimpleDec has a smaller impact on accuracy for Rocket Lake. However, note the significant drop in accuracy for Sandy Bridge.

Next, consider the experiments where we analyze the accuracy of individual components as standalone predictors (rows “only X”). We can see that neither of the components alone can predict throughput accurately. Combining the two most accurate components, Predec+Ports for $BHive_U$ and Precedence+Ports for $BHive_L$, yields significantly higher accuracy but still clearly falls short of FACILE as a whole.

Let us now turn to the experiments where we exclude individual components from FACILE (rows “... w/o X”). On Rocket Lake, we see a notable drop in accuracy when excluding Predec, Ports, and Precedence under $BHive_U$ and/or $BHive_L$. Excluding Dec and LSD has a smaller, yet non-negligible impact on accuracy. In contrast, excluding Issue and DSB has almost no effect on accuracy. For Rocket Lake, individually, these components are thus not required for accurate throughput prediction. However, for Skylake, we see that excluding Issue or DSB leads to a significant drop in accuracy under $BHive_L$, highlighting their importance in general.

6.3. Computational Efficiency

In this section, we study the computational efficiency of FACILE to explore its suitability for use cases that require fast throughput prediction. We measure and compare the execution time of FACILE and the other predictors on both the $BHive_U$ and $BHive_L$ benchmarks.

We conduct our experiments on a Linux workstation with an AMD Ryzen 5900X CPU running at 3.70 GHz with 64 GB of RAM. To ensure consistency of measured execution times, we disable simultaneous multithreading (SMT), set the scaling governor to ‘performance’, and disable dynamic frequency scaling due to Turbo Boost. We run each predictor sequentially on all benchmarks for the Skylake microarchitecture and measure the execution time.

FACILE versus other predictors. Figure 5 shows the execution time of the different predictors on the $BHive_U$ and $BHive_L$ benchmarks. We observe that FACILE is faster than all existing predictors by orders of magnitude. The

closest competitor is Ithema1, which is still almost two orders of magnitude slower than FACILE.

Python-based predictors like OSACA, uiCA, Ithema1 and FACILE incur an overhead every time they are run due to the boot up time of the Python VM. All the other predictors in our experiments are written in C/C++ and do not have this overhead. Both OSACA and uiCA are run once for each benchmark, hence the overhead is incurred for each benchmark. For FACILE, this overhead is only incurred once as we pass all benchmarks to the predictor in a single run. We run Ithema1 in interactive mode, using scripts from [5] that allow us to load the predictor once and keep passing benchmarks to it. Hence, the Python VM bootup time is incurred only once for Ithema1 also. However, even if we deduct the boot up time from OSACA and uiCA’s runtime, they are still slower than FACILE by more than a factor of 100.

Influence of FACILE’s components on efficiency.

We also measure the time taken by FACILE to compute the individual components. First, we run FACILE on all benchmarks with all components deactivated to get the time spent on overhead like parsing the input, disassembling the benchmark, etc. Then, we run individual components on all benchmarks and deduct the overhead runtime to get the time taken to compute each component.

Figure 4 shows the distributions of execution times of FACILE’s components under TP_U and TP_L . The overhead and the Precedence component take up close to 90% of the total execution time in both cases. This indicates that any further efforts to improve the efficiency of FACILE will first need to be focussed on these two factors. Predec and Dec take less time for TP_L than for TP_U as they are often skipped for the loop benchmarks (see Equation 3). The loop benchmarks are generally larger than the unrolled benchmarks, which explains why their analysis takes longer on the average.

6.4. Exploiting Interpretability

In this section, we exploit the interpretability of FACILE to gain insights into the evolution of Intel microarchitectures and the impact of individual components on the overall performance. For brevity, we limit this analysis to TP_U .

Evolution of bottlenecks across microarchitectures.

First, we analyze the evolution of bottlenecks across microarchitectures over the last decade on $BHive_U$ from Sandy

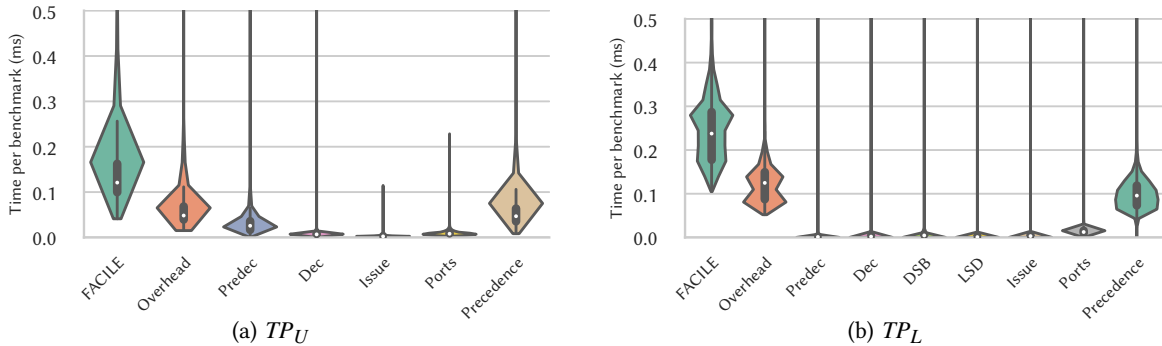


Figure 4: Distributions of execution times of FACILE’s components under TP_U and TP_L .



Figure 5: Efficiency of FACILE compared to other tools.

Bridge via Haswell and Cascade Lake to Rocket Lake. For each *BHive_U* benchmark, we determine the bottleneck component for each of the considered microarchitectures. In case multiple components induce the same throughput, we consider the component that is closest to the front end as the bottleneck, i.e., $\text{Predec} > \text{Dec} > \text{Issue} > \text{Ports} > \text{Precedence}$. The Sankey diagram in Figure 6 shows the share of benchmarks for which a particular component was the bottleneck and how this share evolved across microarchitectures. We can observe that the share of benchmarks that are Predec-bound has increased over time, while the share of benchmarks that are Ports-bound has decreased.

Potential for performance improvement. Finally, we use the model to answer the following counterfactual question: How would performance improve if a particular component were made infinitely fast? Table 4 answers this question for all microarchitectures from Sandy Bridge to Rocket Lake. As expected from the previous experiment, the potential for performance improvement has gradually shifted towards Predec over time. However, as the microarchitectural designs are balanced, performance is usually similarly

TABLE 4: Speedup when idealizing a single component.

	Predec	Dec	Issue	Ports	Precedence
SNB	1.04	1.03	1.00	1.17	1.08
IVB	1.07	1.02	1.00	1.16	1.09
HSW	1.07	1.03	1.00	1.13	1.08
BDW	1.08	1.03	1.00	1.12	1.08
SKL	1.11	1.00	1.00	1.17	1.11
CLX	1.10	1.00	1.00	1.15	1.09
ICL	1.11	1.01	1.00	1.08	1.12
TGL	1.11	1.01	1.00	1.08	1.12
RKL	1.12	1.01	1.00	1.10	1.10

constrained by multiple components. As a consequence, the potential for performance gains by improving a single component only is limited.

7. Conclusions and Future Work

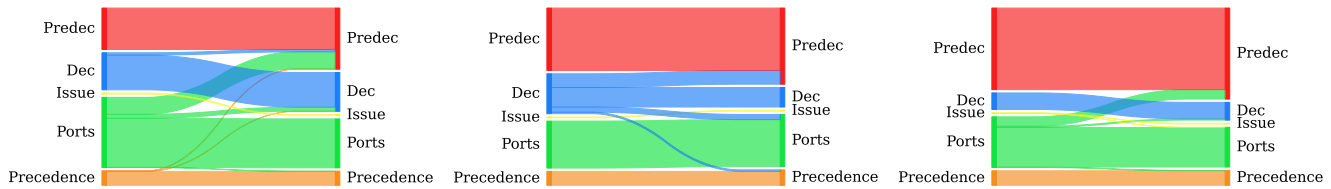
Our experiments demonstrate that FACILE’s compositional analytical model enables highly-accurate, efficient, and interpretable basic-block throughput prediction.

FACILE’s efficiency makes it particularly suitable for use cases that require fast throughput prediction, e.g., in superoptimizers. At first glance, interpretability may seem more relevant for human users than for such automatic tools. However, we believe that interpretability may also be beneficial in settings with no humans in the loop. For example, a superoptimizer could use the model to identify bottlenecks and prioritize optimizations accordingly. Exploring this idea is a direction for future work.

Another direction for future work is to extend FACILE to handle more complex code, e.g., involving branches, and to lift some of the modeling assumptions, e.g., regarding the absence of cache misses. To this end, it may be profitable to combine FACILE’s static predictions with information gathered from dynamic profiling.

Acknowledgments

This project has received funding from the European Research Council under the Horizon 2020 research and innovation programme (grant agreement No. 101020415).



(a) From Sandy Bridge to Haswell

(b) From Haswell to Cascade Lake

(c) From Cascade Lake to Rocket Lake

Figure 6: Evolution of bottlenecks under TP_U from Sandy Bridge to Rocket Lake via Haswell and Cascade Lake.

References

- [1] “MAQAO (modular assembly quality analyzer and optimizer)” [Online]. Available: <http://www.maqao.org>
- [2] “llvm-mca — LLVM machine code analyzer,” 2021. [Online]. Available: <https://llvm.org/docs/CommandGuide/llvm-mca.html>
- [3] A. Abel, “DiffTune-Revisited,” commit c1eef1f. [Online]. Available: <https://github.com/andreas-abel/DiffTune-Revisited>
- [4] —, “uiCA,” commit c1d907e. [Online]. Available: <https://github.com/andreas-abel/uiCA>
- [5] —, “uiCA-eval.” [Online]. Available: <https://github.com/andreas-abel/uiCA-eval>
- [6] —, December 2022. [Online]. Available: <https://uops.info/instructions.xml>
- [7] —, “DiffTune revisited: A simple baseline for evaluating learned llvm-mca parameters,” in *Machine Learning for Computer Architecture and Systems 2022*, June 2022. [Online]. Available: <https://openreview.net/pdf?id=dw4evoj6AE>
- [8] A. Abel and J. Reineke, “uops.info: Characterizing latency, throughput, and port usage of instructions on Intel microarchitectures,” in *Proceedings of the Twenty-Fourth International Conference on Architectural Support for Programming Languages and Operating Systems (ASPLOS)*, Providence, RI, USA, April 13-17, 2019, ser. ASPLOS ’19. ACM, 2019, pp. 673–686. [Online]. Available: <http://doi.acm.org/10.1145/3297858.3304062>
- [9] —, “uiCA: Accurate throughput prediction of basic blocks on recent Intel microarchitectures,” in *ICS ’22: 2022 International Conference on Supercomputing, Virtual Event, USA, June 27-30, 2022*, ser. ICS ’22, L. Rauchwerger, K. Cameron, D. S. Nikolopoulos, and D. Pneumatikatos, Eds. ACM, June 2022, pp. 1–12. [Online]. Available: <https://dl.acm.org/doi/pdf/10.1145/3524059.3532396>
- [10] T. Austin, E. Larson, and D. Ernst, “SimpleScalar: An infrastructure for computer system modeling,” *Computer*, vol. 35, no. 2, pp. 59–67, 2002. [Online]. Available: <https://doi.org/10.1109/2.982917>
- [11] N. L. Binkert, B. M. Beckmann, G. Black, S. K. Reinhardt, A. G. Saiti, A. Basu, J. Hestness, D. Hower, T. Krishna, S. Sardashti, R. Sen, K. Sewell, M. S. B. Altamirano, N. Vaish, M. D. Hill, and D. A. Wood, “The gem5 simulator,” *SIGARCH Computer Architecture News*, vol. 39, no. 2, pp. 1–7, 2011. [Online]. Available: <http://doi.acm.org/10.1145/2024716.2024718>
- [12] T. E. Carlson, W. Heirman, and L. Eeckhout, “Sniper: Exploring the level of abstraction for scalable and accurate parallel multi-core simulation,” in *Proceedings of 2011 International Conference for High Performance Computing, Networking, Storage and Analysis*, 2011, pp. 1–12. [Online]. Available: <https://doi.org/10.1145/2063384.2063454>
- [13] A. S. Charif-Rubial, E. Oseret, J. Noudouhouenou, W. Jalby, and G. Lartigue, “CQA: A code quality analyzer tool at binary level,” in *21st International Conference on High Performance Computing (HiPC)*, Dec. 2014, pp. 1–10. [Online]. Available: <http://www.maqao.org/publications/papers/CQA.pdf>
- [14] I. Chaudhary, A. Renda, C. Mendis, and G. Singh, “COMET: X86 cost model explanation framework,” 2023. [Online]. Available: <https://arxiv.org/abs/2302.06836>
- [15] Y. Chen, A. Brahmakshatriya, C. Mendis, A. Renda, E. Atkinson, O. Sykora, S. Amarasinghe, and M. Carbin, “Bhive: A benchmark suite and measurement framework for validating x86-64 basic block performance models,” in *2019 IEEE International Symposium on Workload Characterization (IISWC)*. IEEE, Nov. 2019. [Online]. Available: <http://groups.csail.mit.edu/commit/papers/19/ithemal-measurement.pdf>
- [16] A. Dasdan, “Experimental analysis of the fastest optimum cycle ratio and mean algorithms,” *ACM Trans. Design Autom. Electr. Syst.*, vol. 9, no. 4, pp. 385–418, 2004. [Online]. Available: <https://doi.org/10.1145/1027084.1027085>
- [17] A. Di Biagio, “llvm-mca,” 2018. [Online]. Available: <https://lists.llvm.org/pipermail/llvm-dev/2018-March/121490.html>
- [18] R. A. Howard, *Dynamic Programming and Markov Processes*. Cambridge, MA: MIT Press, 1960.
- [19] R. A. Huff, “Lifetime-sensitive modulo scheduling,” in *Proceedings of the ACM SIGPLAN’93 Conference on Programming Language Design and Implementation (PLDI)*, Albuquerque, New Mexico, USA, June 23-25, 1993, R. Cartwright, Ed. ACM, 1993, pp. 258–267. [Online]. Available: <https://doi.org/10.1145/155090.155115>
- [20] Intel Corporation, “Intel architecture code analyzer.” [Online]. Available: <https://software.intel.com/en-us/articles/intel-architecture-code-analyzer>
- [21] *Intel Architecture Code Analyzer User’s Guide*, Intel Corporation, 2017, Document Number: 321356-001US. [Online]. Available: <https://software.intel.com/content/dam/develop/external/us/en/documents/intel-architecture-code-analyzer-3-0-users-guide-157552.pdf>
- [22] “Mitigations for jump conditional code erratum,” Intel Corporation, Nov. 2019, Document Number: 341810-001. [Online]. Available: <https://www.intel.com/content/dam/support/us/en/documents/processors/mitigations-jump-conditional-code-erratum.pdf>
- [23] “6th generation Intel processor family — Specification update,” Intel Corporation, Dec. 2020, Document Number: 332689-027. [Online]. Available: <https://www.intel.com/content/www/us/en/processors/core/desktop-6th-gen-core-family-spec-update.html>
- [24] M. G. Kendall, “A new measure of rank correlation,” *Biometrika*, vol. 30, no. 1/2, pp. 81–93, 1938. [Online]. Available: <https://doi.org/10.2307/2332226>
- [25] M. Lam, “Software pipelining: An effective scheduling technique for VLIW machines,” in *Proceedings of the ACM SIGPLAN’88 Conference on Programming Language Design and Implementation (PLDI)*, Atlanta, Georgia, USA, June 22-24, 1988, R. L. Wexelblat, Ed. ACM, 1988, pp. 318–328. [Online]. Available: <https://doi.org/10.1145/53990.54022>
- [26] C. Lattner and V. Adve, “LLVM: A compilation framework for lifelong program analysis & transformation,” in *Proceedings of the International Symposium on Code Generation and Optimization: Feedback-directed and Runtime Optimization*, ser. CGO ’04. Washington, DC, USA: IEEE Computer Society, 2004, pp. 75–86. [Online]. Available: <http://dl.acm.org/citation.cfm?id=977395.977673>

- [27] J. Laukemann, J. Hammer, G. Hager, and G. Wellein, "Automatic throughput and critical path analysis of x86 and ARM assembly kernels," in *IEEE/ACM Performance Modeling, Benchmarking and Simulation of High Performance Computer Systems (PMBS)*, Nov. 2019. [Online]. Available: <https://doi.org/10.1109/PMBS49563.2019.00006>
- [28] J. Laukemann, J. Hammer, J. Hofmann, G. Hager, and G. Wellein, "Automated instruction stream throughput prediction for Intel and AMD microarchitectures," in *IEEE/ACM Performance Modeling, Benchmarking and Simulation of High Performance Computer Systems (PMBS)*. Los Alamitos, CA, USA: IEEE Computer Society, Nov. 2018, pp. 121–131. [Online]. Available: <https://doi.org/10.1109/PMBS.2018.8641578>
- [29] Z. Liu, S. Mada, and J. Regehr, "Minotaur: A SIMD-oriented synthesizing superoptimizer," *CoRR*, vol. abs/2306.00229, 2023. [Online]. Available: <http://arxiv.org/abs/2306.00229>
- [30] G. H. Loh, S. Subramaniam, and Y. Xie, "Zesto: A cycle-level simulator for highly detailed microarchitecture exploration," in *Proceedings of the IEEE International Symposium on Performance Analysis of Systems and Software (ISPASS)*, 2009, pp. 53–64. [Online]. Available: <https://doi.org/10.1109/ISPASS.2009.4919638>
- [31] A. McGovern and J. E. B. Moss, "Scheduling straight-line code using reinforcement learning and rollouts," in *Advances in Neural Information Processing Systems 11, [NIPS Conference, Denver, Colorado, USA, November 30 - December 5, 1998]*, M. J. Kearns, S. A. Solla, and D. A. Cohn, Eds. The MIT Press, 1998, pp. 903–909.
- [32] C. Mendis and S. Amarasinghe, "GoSLP: Globally optimized superword level parallelism framework," *Proc. ACM Program. Lang.*, vol. 2, no. OOPSLA, oct 2018. [Online]. Available: <https://doi.org/10.1145/3276480>
- [33] C. Mendis, A. Renda, S. Amarasinghe, and M. Carbin, "Ithemal: Accurate, portable and fast basic block throughput estimation using deep neural networks," in *Proceedings of the 36th International Conference on Machine Learning*, ser. Proceedings of Machine Learning Research, vol. 97. Long Beach, California, USA: PMLR, Jun. 2019, pp. 4505–4515. [Online]. Available: <http://proceedings.mlr.press/v97/mendis19a.html>
- [34] A. Patel, F. Afram, S. Chen, and K. Ghose, "MARSS: A full system simulator for multicore x86 CPUs," in *Proceedings of the 48th Design Automation Conference*, 2011, pp. 1050–1055. [Online]. Available: <https://doi.org/10.1145/2024724.2024954>
- [35] P. M. Pothilimthana, A. Thakur, R. Bodik, and D. Dhurjati, "Scaling up superoptimization," in *Proceedings of the Twenty-First International Conference on Architectural Support for Programming Languages and Operating Systems, ASPLOS 2016, Atlanta, GA, USA, April 2-6, 2016*, T. Conte and Y. Zhou, Eds. ACM, 2016, pp. 297–310. [Online]. Available: <https://doi.org/10.1145/2872362.2872387>
- [36] A. Pohl, B. Cosenza, and B. Juurlink, "Portable cost modeling for auto-vectorizers," in *2019 IEEE 27th International Symposium on Modeling, Analysis, and Simulation of Computer and Telecommunication Systems (MASCOTS)*, 2019, pp. 359–369. [Online]. Available: <https://doi.org/10.1109/MASCOTS.2019.00046>
- [37] —, "Vectorization cost modeling for NEON, AVX and SVE," *Performance Evaluation*, vol. 140-141, p. 102106, 2020. [Online]. Available: <https://www.sciencedirect.com/science/article/pii/S0166531620300262>
- [38] B. R. Rau, "Iterative modulo scheduling: an algorithm for software pipelining loops," in *Proceedings of the 27th Annual International Symposium on Microarchitecture, San Jose, California, USA, November 30 - December 2, 1994*, H. Mulder and M. K. Farrens, Eds. ACM / IEEE Computer Society, 1994, pp. 63–74. [Online]. Available: <https://doi.org/10.1109/MICRO.1994.717412>
- [39] A. Renda, M. Carbin, and Y. Chen, "DiffTune," commit 9992f69. [Online]. Available: <https://github.com/ithemal/DiffTune>
- [40] —, "Ithemal," commit 47a5734. [Online]. Available: <https://github.com/ithemal/Ithemal>
- [41] A. Renda, Y. Chen, C. Mendis, and M. Carbin, "DiffTune: Optimizing CPU simulator parameters with learned differentiable surrogates," in *53rd Annual IEEE/ACM International Symposium on Microarchitecture (MICRO)*, Oct. 2020, pp. 442–455. [Online]. Available: <https://doi.org/10.1109/MICRO50266.2020.00045>
- [42] M. T. Ribeiro, S. Singh, and C. Guestrin, "Anchors: High-precision model-agnostic explanations," in *Proceedings of the AAAI conference on artificial intelligence*, vol. 32, no. 1, 2018. [Online]. Available: <https://www.aaai.org/ocs/index.php/AAAI/AAAI18/paper/view/16982>
- [43] F. Ritter and S. Hack, "AnICA: analyzing inconsistencies in microarchitectural code analyzers," *Proceedings of the ACM on Programming Languages*, vol. 6, no. OOPSLA2, pp. 1–29, 2022. [Online]. Available: <https://doi.org/10.1145/3563288>
- [44] D. Sanchez and C. Kozyrakis, "ZSim: Fast and accurate microarchitectural simulation of thousand-core systems," in *Proceedings of the 40th Annual International Symposium on Computer Architecture*, ser. ISCA '13. New York, NY, USA: ACM, 2013, pp. 475–486. [Online]. Available: <http://doi.acm.org/10.1145/2485922.2485963>
- [45] R. Sasnauskas, Y. Chen, P. Collingbourne, J. Ketema, J. Taneja, and J. Regehr, "Souper: A synthesizing superoptimizer," *CoRR*, vol. abs/1711.04422, 2017. [Online]. Available: <http://arxiv.org/abs/1711.04422>
- [46] E. Schkufza, R. Sharma, and A. Aiken, "Stochastic superoptimization," in *Architectural Support for Programming Languages and Operating Systems, ASPLOS 2013, Houston, TX, USA, March 16-20, 2013*, V. Sarkar and R. Bodik, Eds. ACM, 2013, pp. 305–316. [Online]. Available: <https://doi.org/10.1145/2451116.2451150>
- [47] —, "Stochastic program optimization," *Commun. ACM*, vol. 59, no. 2, pp. 114–122, 2016. [Online]. Available: <https://doi.org/10.1145/2863701>
- [48] M. Stephenson, S. P. Amarasinghe, M. C. Martin, and U. O'Reilly, "Meta optimization: improving compiler heuristics with machine learning," in *Proceedings of the ACM SIGPLAN 2003 Conference on Programming Language Design and Implementation 2003, San Diego, California, USA, June 9-11, 2003*, R. Cytron and R. Gupta, Eds. ACM, 2003, pp. 77–90. [Online]. Available: <https://doi.org/10.1145/781131.781141>
- [49] O. Šykora, P. M. Pothilimthana, C. Mendis, and A. Yazdanbakhsh, "GRANITE: A graph neural network model for basic block throughput estimation," in *2022 IEEE International Symposium on Workload Characterization (IISWC)*. IEEE, 2022, pp. 14–26. [Online]. Available: <https://doi.org/10.1109/IISWC55918.2022.00012>
- [50] M. Trofin, Y. Qian, E. Brevdo, Z. Lin, K. Choromanski, and D. Li, "MLGO: a machine learning guided compiler optimizations framework," *CoRR*, vol. abs/2101.04808, 2021. [Online]. Available: <https://arxiv.org/abs/2101.04808>
- [51] M. T. Yourst, "PTLsim: A cycle accurate full system x86-64 microarchitectural simulator," in *2007 IEEE International Symposium on Performance Analysis of Systems & Software*. IEEE, 2007, pp. 23–34. [Online]. Available: <https://doi.org/10.1109/ISPASS.2007.363733>